https://www.scirp.org/journal/jbise
J. Biomedical Science and Engineering,
2025, Vol. 18, (No. 8), pp: 317-327

Brain Functional Connectivity Network (BFCN) Analysis Using Scalp-Recorded EEGs after Human Papilloma Virus Vaccination

Toshiaki Hirai[1], Toshimasa Yamazaki[2], Chisho Takeoka[3], Yoshiyuki Kuroiwa[1], Kimihiro Fujino[1]

[1]University Hospital, Mizonokuchi Teikyo University School of Medicine, Kawasaki, Japan; [2]Department of Computer Science and Systems Engineering, Kyushu Institute of Technology, Fukuoka, Japan; [3]Graduate School of Computer Science and Systems Engineering, Kyushu Institute of Technology, Fukuoka, Japan

Correspondence to: Toshiaki Hirai, hirait@med.teikyo-u.ac.jp; Toshimasa Yamazaki, tymzk@bio.kyutech.ac.jp
Keywords: HANS (Human Papilloma Virus Vaccination Associated Neuro-Immunopathic Syndrome), EEGs (Electroencephalograms), Functional Connectivity, Network Properties
Received: July 2, 2025 **Accepted:** August 11, 2025 **Published:** August 14, 2025

ABSTRACT

Background/Objectives: HANS (human papillomavirus vaccination-associated neuroimmunopathic syndrome) is a type of adverse reaction to HPV vaccination that causes cognitive dysfunction. Human brain function can be represented by functional connectivity and the Brain Functional Connectivity Network (BFCN), which are constructed by scalp-recorded electroencephalograms (EEGs). Functional connectivity and BFCN are used to estimate functional efficiency. The effects of cognitive dysfunction on network properties have been reported. However, network properties in HANS patients are incompletely understood. In this study, we examined (1) identifiability between HANS patients and young controls and (2) the impact of cognitive dysfunction due to HANS on BFCN for five frequency bands. *Methods*: 16-ch EEGs were recorded in a resting state with eyes closed for 14 HANS patients and 12 young controls. We used Synchronization Likelihood (SL) as measured functional connectivity, which is used for classification by machine learning and for the construction of BFCN for five frequency bands. In (1), SL values were used as features for classification. Accuracies were calculated by leave-one-out cross-validation. Accuracies for five frequency bands were compared to that of random prediction. In (2), clustering coefficient, characteristic path length, and small-worldness of BFCN were compared between HANS patients and young controls. *Results*: Our study revealed (1) high accuracies were illustrated for lower alpha and theta bands and (2) a significant decrease compared to controls in small-worldness in HANS patients for the gamma band. *Conclusion*: Our study shows identifiability between HANS patients and young controls. In

addition, changes in network characteristics based on functional connectivity are relevant to cognitive dysfunction in HANS.

1. INTRODUCTION

The vaccination with the human papillomavirus vaccine (HPV) is promoted worldwide to prevent cervical cancer. The HPV vaccine was created to prevent HPV infection in the cervix and reduce the incidence of cervical cancer. However, it was feared to be life-threatening for young women. The medical term HPVV-associated neuroimmune disorder syndrome (HANS) was proposed in 2014 [1]. Various unexpected symptomatic complexes (SC) have been observed after HPV infection in young women. Thousands of adverse drug reaction (ADR) cases have been reported to the MHLW in Japan [2]. HANS is characterized by disrupted neuroendocrine homeostasis and decreased blood flow in the cingulate gyrus and thalamus. HANS patients often show cognitive disorders such as prosopagnosia, kanji writing disorder, topographical disorientation, and hemispatial neglect.

Hypothalamic dysfunction in HANS patients has been reported [2, 3]. The hypothalamus is the center of the autonomic nervous system that controls vital phenomena and is the center of coordination of the entire cerebral cortex. Dysfunction of the hypothalamus could affect the function of the entire cortex.

There are no neurophysiological markers specific to HANS. In the field of functional imaging, Matsudaira *et al.* performed positron emission tomography (PET) examinations on 12 patients with HPV-related adverse reactions and reported neuroinflammation and decreased cerebral blood flow in the thalamus, limbic system, and brainstem regions [4].

The problem with this study is that there are few pathological reports, and it is unclear whether the cause is inflammation caused by an immune response or a functional abnormality. In addition, there is no way to confirm whether the abnormalities existed before the vaccination, even if abnormalities are found. It could be a research issue. However, since people who had some kind of health abnormality before the vaccination cannot be diagnosed with HANS (they are excluded), this study was conducted with the idea that the abnormalities and pathology can be considered in the differences between the control group. Although there have been reports of side effects from HPV vaccination [5], this report was not written to deny the vaccination, but rather was conducted to examine whether there were any neurophysiological abnormalities in the brain.

Elucidation of brain function in HANS patients is important for the diagnosis, prevention, and treatment of HANS. Brain Functional Connectivity Network (BFCN) [6] reflects complex brain function as a network. Various data-driven approaches have been used to assess brain function and connectivity in the study of statistical dependencies between recorded EEG signals. Chiarion *et al.* categorize various pairwise and multivariate, as well as directed and undirected connectivity metrics in the time, frequency, and information-theoretic domains in their technical description [7].

Highly accurate classification by machine learning using functional connectivity has been reported. Raveendran *et al.* applied a connectivity calculation method called amplitude envelope correlation (AEC) and showed highly accurate classification of four consciousness states (coma, UWS, MCS, and healthy subjects) [8]. In addition, it has been suggested that it would be possible to classify between the two tasks through a classifier trained on features extracted from brain connectivity analysis. Antonacci *et al.* demonstrated high accuracy in classifying right-hand motor imagery (HAND) and foot motor imagery (FOOT) using features derived from connectivity analysis [9].

To define functional connectivity, Synchronization Likelihood (SL) [10, 11] was applied. SL is a measure of synchronization between two time series that is sensitive to linear and nonlinear independence. Mumtaz *et al.* created a machine learning framework using functional connectivity for the classification of patients with major depressive disorder and healthy controls [12]. The results showed highly accurate discrimination. SL was used in this study to compute functional connectivity. BFCN is constructed by functional connectivity. In BFCN, complex brain functions are reflected as networks. It represents the unique function of each

brain region and the sharing of information between different regions. BFCN is composed of nodes and edges. Nodes essentially represent individual neurons or aggregates of them, and can be mapped to each brain region responsible for functional responsibilities. Edges defined between one of the pair of nodes is a model of a nerve fiber. Quantitative connectivity was introduced to give edges a relationship between nodes. BFCN is defined by graph theory and reflects connectivity between brain regions. Local and global connectivity of the BFCN is associated with cognitive function, and changes in network properties have been reported in brain disorders with cognitive dysfunction compared to healthy controls [13-16] and in aging compared to younger [17, 18].

We hypothesized that functional connectivity and BFCN may reflect cognitive dysfunction in HANS patients. The purpose of this study is to examine identifiability between HANS patients and younger controls based on SL and the network properties of BFCN in HANS patients constructed based on SL computed from scalp-recorded electroencephalograms (EEGs). Much research has been conducted to elucidate the pathomechanisms and to objectively determine disability [3, 5, 19, 20]. However, few studies have examined changes in network properties in cognitive dysfunction that develops after vaccination. Although there is a possibility of an impact on the function of the entire cerebral cortex in HANS patients, the construction of networks using EEG data recorded in the cerebral cortex and the validation of their properties have not been conducted. EEG is easy to measure, inexpensive, and places little burden on patients. Considering the application of this research to clinical settings, it is important to clarify significant differences and to demonstrate a high accuracy for classification between HANS patients and healthy controls using EEG.

In this study, we expect that machine learning using functional connectivity would enable accurate classification of HANS patients and young controls. In addition, we hypothesized that significant differences in network properties would reflect differences in network structure by comparing the BFCN of HANS patients and young controls.

2. MATERIALS AND METHODS

2.1. EEG Measurement

Subjects consisted of 14 HANS patients (female: 14, mean: 22.79 years, standard deviation: 4.49 years) and 12 young controls (male: 7, female: 5, mean: 27.92 years, standard deviation: 10.94 years). HANS patients had involuntary movements and seizures and were deemed to require electroencephalography (EEG) measurement by neurologists. Young controls visited the hospital at the same time as the HANS patients. They had symptoms such as loss of consciousness and seizures, and a neurologist determined that an EEG measurement was necessary, but they were not diagnosed with HANS. These subjects were chosen as the control because it was assumed that it would be difficult to collect the same number of healthy individuals with no symptoms as HANS patients during the study period. Written informed consents were obtained from all participants. The study protocol, including all EEG data analysis, was approved by Research Ethics Committee, Faculty of Medicine, Teikyo University. EEG measurements were performed at Mizonokuchi Hospital, Teikyo University School of Medicine, through a Nihon Kohden EEG-1224. The device was equipped with 16 Ag/AgCl electrodes (channels) (a Nihon Kohden H503A). Electrodes were attached at Fp1, Fp2, F3, F4, C3, C4, P3, P4, O1, O2, F7, F8, T3, T4, T5, and T6 based on the international 10 - 20 system. In addition to the 16 electrodes, A1 and A2 (reference electrodes) were attached to both earlobes. The sampling frequency was set to 500 Hz and a low-pass filter (=120 Hz), except for the Japanese electrical power noise (50 Hz), was set to removed artifacts. All subjects were asked to lie on their backs in a resting position with eyes closed for at least 5 minutes. All EEG data were checked with EEGLAB (provided by the Swartz Center for Computational Neuroscience). For all subjects, EEG data from the second to third minute of measurement were used as stable EEG data for analysis. All EEG data were reconstructed by Fourier transform and inverse Fourier transform into 5 frequency bands: theta (4 - 8 Hz), lower alpha (8 - 10 Hz), upper alpha (10 - 13 Hz), beta (13 - 30 Hz), and gamma (30 - 45 Hz).

2.2. Synchronization Likelihood (SL)

After EEG data processing, Synchronization Likelihood (SL) was applied between all two electrodes in each of the five frequency bands [10, 11]. The SL value is a measure of synchronization between the two channels, which avoids bias due to the degrees of freedom of the interacting subsystems and can deal with non-stationary dynamics. The basic principle of SL is to divide each time series into a series of "patterns" (short portions of the time series containing several cycles of the main frequency) and to search for repetitions of these patterns [11].

Figure 1 shows an outline of calculation of SL at reference time i. The calculation consisted of following steps: First, the state vector of channel k at reference time i was defined as follows:

$$X_{k,i} = \left(x_{k,i}, x_{k,i+L}, x_{k,i+2*L}, \cdots, x_{k,i+(m-1)*L} \right) \tag{1}$$

where $x_{k,i}$ is the time series of channel k. L is the lag and m is the dimension of the embedding vector in state space. $L*(m-1)$ is the length of state vector. L, m, and $L*(m-1)$ were defined as follows:

$$L = fs/(3*HF) \tag{2}$$

$$L*(m-1) = fs/LF \leftrightarrow m = 3*HF/LF + 1 \tag{3}$$

where fs is the sampling frequency in Hz. In this study, fs was defined as 500 Hz. HF and LF are the highest and lowest frequency of the frequency band of interest.

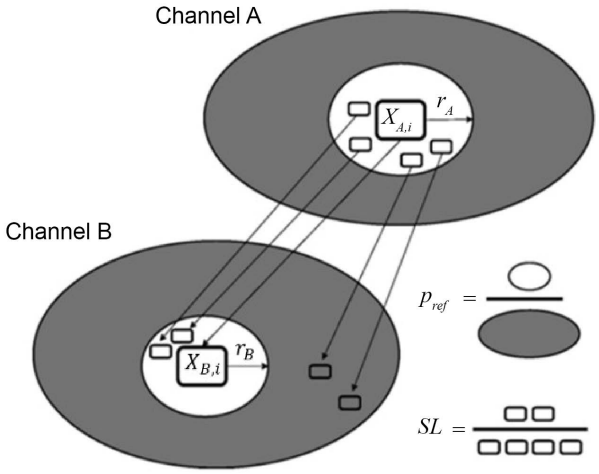

Figure 1. An outline of calculation of SL. reproduced from T. Montez *et al.* (2006) with permission.

Second, reference vector $X_{A,i}$ and vectors $X_{A,j}$ were constructed ranging from $i - W_2/2$ to $i - W_2/2$ and from $i + W_1/2$ to $i + W_2/2$ in steps of $1/fs$, respectively. Here, W_1 and W_2 are defined as follows:

$$W_1 = 2*L*(m-1) \tag{4}$$

$$n_{rec} = [W_2 - W_1 + 1]*p_{ref} \leftrightarrow W_2 = (n_{rec}/p_{ref}) + W_1 - 1 \tag{5}$$

In this study, $n_{rec} = 10$ and $p_{ref} = 0.01$.

Third, SL_i between channels A and B at time i was calculated as follows:

$$SL_i = n_{AB}/n_{rec} \tag{6}$$

where n_{AB} is the number of simultaneous repetitions in channels A and B, and is defined as follows:

$$n_{AB} = \sum_{j=i-W_1/2}^{i-W_1/2} n + \sum_{j=i+W_1/2}^{i+W_2/2} n$$

$$n = \theta\left(r_{A,i} - \left|X_{A,i} - X_{A,j}\right|\right)\theta\left(r_{B,i} - \left|X_{B,i} - X_{B,j}\right|\right)$$

$$\theta(x) = \begin{cases} 1 & \text{if } x \geq 0 \\ 0 & \text{if } x < 0 \end{cases} \tag{7}$$

These three steps were repeated to obtain SL time series. To calculate SL time series, reference time i increases with 32 ms increment. The first and last data points of SL time series were deleted (40 data points for other frequency bands). SL value is the average of SL time series after deletion of data points.

For each functional connectivity, SL values consisting of data from 26 subjects was compared to the same number of 0. In this study, no functional connectivity was defined that SL value was 0. T-tests were performed with the null hypothesis "there is no functional connectivity between EEG signal pairs." The null hypothesis has been rejected for all frequency bands.

BFCN consisted of nodes and edges [3]. In this study, nodes correspond to electrodes where EEGs were recorded. Functional connectivity was represented by SL value. SL values of ${}_{16}C_2 = 120$ pairs of nodes were calculated because EEGs were recorded at 16 electrodes. In addition, 120 SL values $SL_{ij}\left(i < j; i, j = 1, 2, \cdots, 16\right)$ were standardized and exponentially transformed ($\exp\left(Z\left(SL_{ij}\right)\right)$).

2.3. Identifiability

To verify identifiability between HANS patients and young controls, accuracies of classification were evaluated by machine learning. Leave-one-out cross validation (LOOCV) was applied in this study since the number of subjects is relatively small. We used the gradient boosting for discrimination between HANS patients and young control. This algorithm is one of the ensemble learning methods in machine learning, a method of combining weak learners to build a strong learner. SL_{ij} and $\exp\left(Z\left(SL_{ij}\right)\right)$ were used as features for each frequency band. Finally, the accuracies were calculated. Accuracies were obtained according to,

$$\text{Accuracy} = \left(\text{TP} + \text{TN}\right)/\left(\text{TP} + \text{TN} + \text{FP} + \text{FN}\right) \tag{8}$$

where TP, TN, FP, and FN mean the number of true positives, true negatives, false positives, and false negatives, respectively.

To define high accuracy of classification, random prediction of 26 subjects was executed. 100,000 random predictions were run and a distribution chart of the accuracy was created. We defined the top 2% of accuracies as high accuracy. The top 2% of accuracies was 19/26 = 73.1% or more (**Figure 2**).

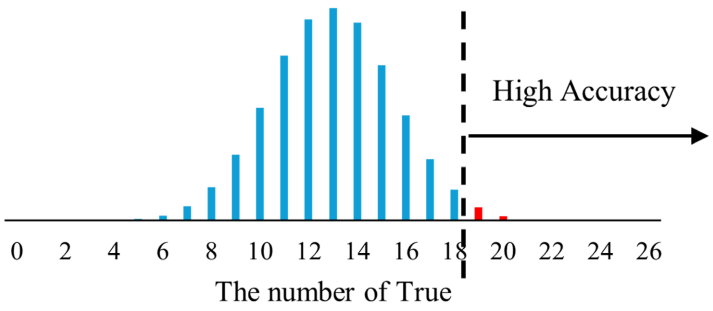

Figure 2. Distribution of random predictions with 26 subjects. Vertical axis is frequency. Horizontal axis is the number of true. Red bars depict high accuracy.

2.4. Network Indices

In this study, BFCN was constructed. BFCN is composed of nodes and edges. Nodes refer to 16 electrodes. Edges between pairs of nodes were quantified by SL_{ij} or $\exp\left(Z\left(SL_{ij}\right)\right)$. Clustering coefficient (C), characteristic path length (L) and small-worldness (SW) were calculated as network indices. These were calculated to each subject and each frequency band.

C represents the local connectivity of the network and has been interpreted as a measure of resilience to random error [18]:

$$C = \left(1/N\right) * \sum_{i=1}^{N} \left(\sum_{k \neq i} \sum_{l \neq i, l \neq k} w_{ik} w_{il} w_{kl} \Big/ \sum_{k \neq i} \sum_{l \neq i, l \neq k} w_{ik} w_{il} \right) \tag{9}$$

where w_{ik} represents the weights of edges between node i and k. N is the number of nodes. C was calculated based on whether there was edge between two nodes connected to node i.

L represents the global connectivity of the network and indicates how well integrated a graph is, and how easy it is to transport information or other entities in the network [21]:

$$L = 1 \Big/ \left(N * \left(N - 1 \right) \right) \sum_{i, j \in N, i \neq j} d_{i,j} \tag{10}$$

where d_{ij} is the shortest path length between i and j. N is the number of nodes. L is the average shortest path length any two nodes. In this study, L was calculated by the average.path.length function (in the igraph package) in R.

SW represents the efficacy of network information transmission [22]:

$$SW = \left(C/C_{rand}\right) \Big/ \left(L/L_{rand}\right) \tag{11}$$

where C_{rand} and L_{rand} denote C and L averaged over an ensemble of 50 random networks that were derived from the original networks by randomly reshuffling the edge weights (SL_{ij} or $\exp\left(Z\left(SL_{ij}\right)\right)$) [21].

To compare C, L, and SW between HANS patients and young controls, we performed two-sided t-tests. HANS patients and young controls were compared for 3 indices and for all 5 frequency bands.

3. RESULT

3.1. Identifiability by Evaluation of Classification Accuracy

Classification of SL_{ij} or $\exp\left(Z\left(SL_{ij}\right)\right)$ using gradient boosting algorithm, accuracies of LOOCV were calculated for each frequency band. The results were reported in **Table 1**. This table shows high accuracies using $\exp\left(Z\left(SL_{ij}\right)\right)$ for theta and lower alpha bands. Accuracies were 73.1% and 76.9%, respectively (**Table 1**).

Table 1. Accuracies of LOOCV.

	theta	lower alpha	upper alpha	beta	gamma
SL_{ij}	0.308	0.269	0.231	0.308	0.615
$\exp\left(Z\left(SL_{ij}\right)\right)$	0.731	0.769	0.462	0.500	0.154

3.2. Significant Differences of Network Indices

Clustering coefficients (C), characteristic path length (L) and small-worldness (SW) of BFCN by SL_{ij} or $\exp\left(Z\left(SL_{ij}\right)\right)$ were calculated in young controls and HANS patients (**Table 2**, **Table 3**). Significant

differences were verified using p-values (p = 0.05). The result showed significant differences at SW using $\exp\left(Z\left(SL_{ij}\right)\right)$ for gamma band (p = 0.024) (Figure 3).

Table 2. Network indices for HANS patients and young controls using SL_{ij}.

Frequency band	Graph Index	HANS (N = 14)		Control (N = 12)		p-value
		Mean	SD	Mean	SD	
theta	C	0.598	0.011	0.600	0.018	0.714
	L	0.883	0.012	0.882	0.008	0.839
	SW	1.000	0.000	1.000	0.000	-
lower alpha	C	0.334	0.011	0.334	0.013	0.952
	L	0.820	0.014	0.823	0.012	0.526
	SW	1.000	0.000	1.000	0.000	-
upper alpha	C	0.286	0.006	0.286	0.010	0.978
	L	0.827	0.013	0.827	0.019	0.975
	SW	1.000	0.000	1.000	0.000	0.336
beta	C	0.267	0.012	0.266	0.008	0.907
	L	0.826	0.038	0.817	0.030	0.529
	SW	1.000	0.000	1.000	0.000	0.167
gamma	C	0.138	0.008	0.141	0.006	0.241
	L	0.811	0.037	0.829	0.018	0.141
	SW	1.000	0.001	1.000	0.000	0.261

Table 3. Network indices for HANS patients and young controls using $\exp\left(Z\left(SL_{ij}\right)\right)$.

Frequency band	Graph Index	HANS (N = 14)		Control (N = 12)		p-value
		Mean	SD	Mean	SD	
theta	C	6.398	4.614	8.973	16.99	0.634
	L	0.122	0.035	0.128	0.047	0.758
	SW	0.779	0.077	0.732	0.063	0.110
lower alpha	C	4.762	2.969	3.178	0.530	0.080
	L	0.151	0.043	0.167	0.064	0.493
	SW	0.779	0.047	0.758	0.128	0.613

Continued

upper alpha	C	4.390	3.797	3.596	0.809	0.474
	L	0.188	0.084	0.174	0.051	0.612
	SW	0.765	0.159	0.771	0.126	0.913
beta	C	4.775	3.419	4.402	1.593	0.729
	L	0.270	0.083	0.255	0.083	0.666
	SW	0.655	0.155	0.677	0.182	0.760
gamma	C	10.17	14.82	4.719	1.123	0.209
	L	0.341	0.122	0.275	0.072	0.117
	SW	0.629	0.107	0.733	0.103	0.024

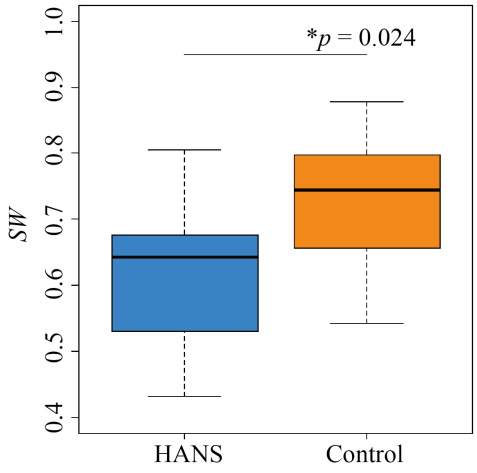

Figure 3. Small-worldness (SW) using $\exp\left(Z\left(SL_{ij}\right)\right)$ for gamma band. Blue box represents HANS patients, and orange one represents young controls. One asterisk (*) represents a significant difference ($p < 0.05$).

4. DUSCUSSION

The purpose of this study was to examine network properties in BFCN of HANS patients with cognitive dysfunction by comparing them with young controls. We found identifiability for theta and lower alpha band and structural changes for gamma bands in BFCN of HANS patients. In general, neuropathy after HPV vaccination is often considered psychogenic, but results in our study were not necessarily the case.

Functional connectivity between brain regions was quantified by synchronization calculated by SL. SL is associated with cognitive dysfunction. Stam *et al.* showed that SL values in Alzheimer's disease patients were significantly different with young controls and mild cognitive impairment (MCI) patients, which correlated with lower Mini-Mental State Examination (MMSE) scores [4]. Teng *et al.* examined EEG synchronization at rest and during working memory tasks and reported a significant decrease in synchronization in the elderly compared to younger patients [18]. Given these studies, cognitive dysfunction would be associated with functional connectivity.

To verify identifiability by using values of functional connectivity, LOOCV was applied and calculated accuracies. High accuracies were illustrated for theta and lower alpha bands. In random prediction of 26 Subjects, the Probability of getting 73.1% and 76.9% accuracy is less than 2% and 0.5%, respectively. Hence, functional connectivity would be useful for identifiability between HANS patients and young controls.

We examined changes in the network properties of HANS patients based on graph theory. Calculations of C, L, and SW have also received attention in studies supporting cognitive dysfunction. Network properties are characterized by these indices. Stam *et al.* and Sanz-Arigita *et al.* calculated these indices in BFCN of Alzheimer's disease patients and reported significant differences from healthy controls [14, 16]. Gaál *et al.* reported that the brain networks of the elderly alter network indices compared to youngers [17]. However, their study shows altered these indices in young or elderly healthy individuals and in dementia patients. In this study, we applied the standardized and exponentially transformed SL as theirs to examine network properties in HANS patients. We observed changes in these indices of BFCN in HANS patients compared to younger controls. We found a significant differences in SW for gamma band of BFCN in HANS patients. This result suggests that cognitive function in HANS could also be explained by BFCN construction by SL and is associated with changes in functional brain organization. Furthermore, SW are associated with the efficacy of network information transmission. It is suggested that cognitive dysfunction in HANS patients, such as prosopagnosia, kanji writing disorder, topographical disorientation, and hemispatial neglect, is sensitive to changes in connectivity to the overall network. This could be explained by the fact that HANS is associated with hypothalamic dysfunction [2, 3] and that the hypothalamus is the center of coordination of the entire cortex and dysfunction of the hypothalamus can affect the function of the entire cortex.

Several limitations of this study are mentioned. First, the small number of EEG channels in this study may limit the spatial resolution and the potential volume conduction effect of the EEG sensor may affect the results. To minimize these limitations, the electrodes were placed according to the international 10 - 20 system, which is recommended as an international standard and is based on the anatomical parts of the brain.

Another limitation is the time required to extract EEG data with non-stationarity. In this study, we used a minute of EEG data for analysis to reduce data variability and suppress noise and artifacts. ADF test was performed. This test is statistical test to examine whether time series data has stationarity. Significant differences were confirmed for all frequency bands, indicating stationarity.

Then, spurious connections may occur at the SL value. When two time series data are both influenced by a third time series data, it is possible to detect false causal relationship between the two time series data [23]. One approach to this problem in this study is to define the third EEG data as a latent variable and analyze the cross-correlation function with each EEG data. Cross-correlation function is one of the measures of interdependence between two time series. The cross-correlation function measures the linear correlation between two time series data as a function of their delay time, which is of interest because such a time delay may reflect a causal relationship between the signals [24]. This approach would be the resolution of limitations by inferring casual relationships at least partially revealing possible spurious connections. In this study, high accuracy was demonstrated by machine learning for automatic diagnosis using SL as input data as in [12]. The approach based on SL analysis is simple and efficient for highly accurate classification of HANS. Identifiability and significant differences in network indices were shown. Therefore, these were considered as the results of this study.

Finally, there is concern about the inclusion of male participants in the control group. During the study period, there were few female patients who met the criteria, so male patients were included. Gong *et al.*, indicated that it should be mandatory to take gender-related cognitive differences into account when designing experiments or interpreting results of brain connectivity/network in health and disease [25]. To consider this concern, we performed two-sided t-tests between male and female controls to compare functional connectivity and network properties. In the result, there were no significant differences. However, it may be beneficial to include only female participants in the control group. There are also concerns about the insufficient sample size, possibility of independently influencing EEG patterns in control group, and the

assessment of network differences between the HANS patients and young controls based only on resting-state data. To demonstrate the usefulness of the methodology for elucidating brain function, it may be beneficial to consider using a larger sample size in future studies, comparing with healthy individuals with no symptoms at all, including only female participants in the control group, and including additional tasks such as simple Chinese character writing and face recognition tasks.

5. CONCLUSION

Our study demonstrates identifiability by functional connectivity and altered network properties in cognitive dysfunction in HANS patients. Identifiability was indicated for theta and lower alpha bands, while altered network properties were observed in the gamma band by small-worldness. Several studies suggest that the properties of the BFCN are altered by neurodegenerative diseases in dementia patients. Functional connectivity between brain regions and local or global connectivity throughout the network due to BFCN construction may be suitable tools for studying cognitive dysfunction after HPV vaccination.

CONFLICTS OF INTEREST

The authors declare no conflicts of interest regarding the publication of this paper.

REFERENCES

1. Nishioka, K., Yokota, S. and Matsumoto, Y. (2014) Clinical Features and Preliminary Diagnostic Criteria of Human Papillomavirus Vaccination Associated with Neuroimmunopathic Syndrome (HANS). *International Journal of Rheumatic Diseases*, **17**, 29.
2. Kuroiwa, Y., Yokota, S., Nakamura, I., Nakajima, T. and Nishioka, K. (2018) Human Papilloma Virus Vaccination (HPVV)-Associated Neuro-Immunopathic Syndrome (HANS): A Comparative Study of the Symptomatic Complex Occurring in Japanese and Danish Young Females after HPVV. *Autonomic Nervous System*, **55**, 21-30.
3. Hirai, T., Kuroiwa, Y., Hayashi, T., Uchiyama, M., Nakamura, I., Yokota, S., *et al.* (2016) Adverse Effects of Human Papilloma Virus Vaccination on Central Nervous System: Neuro-Endocrinological Disorders of Hypothalamo-Pituitary Axis. *Autonomic Neuroscience*, **201**, 74. https://doi.org/10.1016/j.autneu.2016.09.011
4. Matsudaira, T., Terada, T., Obi, T., Yokokura, M., Takahashi, Y. and Ouchi, Y. (2020) Coexistence of Cerebral Hypometabolism and Neuroinflammation in the Thalamo-Limbic-Brainstem Region in Young Women with Functional Somatic Syndrome. *EJNMMI Research*, **10**, Article No. 29. https://doi.org/10.1186/s13550-020-00617-1
5. Hineno, A., Ikeda, S., Scheibenbogen, C., Heidecke, H., Schulze-Forster, K., Junker, J., Riemekasten, G., Dechend, R., Dragun, D. and Shoenfeld, Y. (2019) Autoantibodies against Autonomic Nerve Receptors in Adolescent Japanese Girls after Immunization with Human Papillomavirus Vaccine. *Annals of Arthritis and Clinical Rheumatology*, **2**, 1014.
6. Sporns, O. (2016) Network of the Brain. MIT Press.
7. Chiarion, G., Sparacino, L., Antonacci, Y., Faes, L. and Mesin, L. (2023) Connectivity Analysis in EEG Data: A Tutorial Review of the State of the Art and Emerging Trends. *Bioengineering*, **10**, Article No. 372. https://doi.org/10.3390/bioengineering10030372
8. Raveendran, S., *et al.* (2025) Functional Connectivity in EEG: A Multiclass Classification Approach for Disorders of Consciousness. *Frontiers in Neuroscience*, **19**, Article ID: 1550581. https://doi.org/10.3389/fnins.2025.1550581
9. Antonacci, Y., Toppi, J., Pietrabissa, A., Anzolin, A. and Astolfi, L. (2024) Measuring Connectivity in Linear Multivariate Processes with Penalized Regression Techniques. *IEEE Access*, **12**, 30638-30652. https://doi.org/10.1109/access.2024.3368637

10. Stam, C.J. and van Dijk, B.W. (2002) Synchronization Likelihood: An Unbiased Measure of Generalized Synchronization in Multivariate Data Sets. *Physica D: Nonlinear Phenomena*, **163**, 236-251. https://doi.org/10.1016/s0167-2789(01)00386-4

11. Montez, T., Linkenkaer-Hansen, K., van Dijk, B.W. and Stam, C.J. (2006) Synchronization Likelihood with Explicit Time-Frequency Priors. *NeuroImage*, **33**, 1117-1125. https://doi.org/10.1016/j.neuroimage.2006.06.066

12. Mumtaz, W., Ali, S.S.A., Yasin, M.A.M. and Malik, A.S. (2017) A Machine Learning Framework Involving EEG-Based Functional Connectivity to Diagnose Major Depressive Disorder (MDD). *Medical & Biological Engineering & Computing*, **56**, 233-246. https://doi.org/10.1007/s11517-017-1685-z

13. Takeoka, C., Yamazaki, T., Kuroiwa, Y., Fujino, K., Hirai, T. and Mizusawa, H. (2023) Functional Connectivity and Small-World Networks in Prion Disease. *IEICE Transactions on Information and Systems*, **106**, 427-430. https://doi.org/10.1587/transinf.2022edl8049

14. Stam, C., Jones, B., Nolte, G., Breakspear, M. and Scheltens, P. (2006) Small-World Networks and Functional Connectivity in Alzheimer's Disease. *Cerebral Cortex*, **17**, 92-99. https://doi.org/10.1093/cercor/bhj127

15. Stam, C.J., Van Der Made, Y., Pijnenburg, Y.A.L. and Scheltens, P. (2003) EEG Synchronization in Mild Cognitive Impairment and Alzheimer's Disease. *Acta Neurologica Scandinavica*, **108**, 90-96. https://doi.org/10.1034/j.1600-0404.2003.02067.x

16. Sanz-Arigita, E.J., Schoonheim, M.M., Damoiseaux, J.S., Rombouts, S.A.R.B., Maris, E., Barkhof, F., *et al.* (2010) Loss of "Small-World" Networks in Alzheimer's Disease: Graph Analysis of fMRI Resting-State Functional Connectivity. *PLOS ONE*, **5**, e13788. https://doi.org/10.1371/journal.pone.0013788

17. Gaál, Z.A., Boha, R., Stam, C.J. and Molnár, M. (2010) Age-Dependent Features of EEG-Reactivity—Spectral, Complexity, and Network Characteristics. *Neuroscience Letters*, **479**, 79-84. https://doi.org/10.1016/j.neulet.2010.05.037

18. Teng, C., Cheng, Y., Wang, C., Ren, Y., Xu, W. and Xu, J. (2018) Aging-Related Changes of EEG Synchronization during a Visual Working Memory Task. *Cognitive Neurodynamics*, **12**, 561-568. https://doi.org/10.1007/s11571-018-9500-6

19. Aratani, S., Fujita, H., Kuroiwa, Y., Usui, C., Yokota, S., Nakamura, I., *et al.* (2016) Murine Hypothalamic Destruction with Vascular Cell Apoptosis Subsequent to Combined Administration of Human Papilloma Virus Vaccine and Pertussis Toxin. *Scientific Reports*, **6**, Article No. 36943. https://doi.org/10.1038/srep36943

20. Ozawa, K., Hineno, A., Kinoshita, T., Ishihara, S. and Ikeda, S. (2017) Suspected Adverse Effects after Human Papillomavirus Vaccination: A Temporal Relationship between Vaccine Administration and the Appearance of Symptoms in Japan. *Drug Safety*, **40**, 1219-1229. https://doi.org/10.1007/s40264-017-0574-6

21. Stam, C.J. and Reijneveld, J.C. (2007) Graph Theoretical Analysis of Complex Networks in the Brain. *Nonlinear Biomedical Physics*, **1**, Article No. 3. https://doi.org/10.1186/1753-4631-1-3

22. Latora, V. and Marchiori, M. (2001) Efficient Behavior of Small-World Networks. *Physical Review Letters*, **87**, Article ID: 198701. https://doi.org/10.1103/physrevlett.87.198701

23. Chen, Y., Bressler, S.L. and Ding, M. (2006) Frequency Decomposition of Conditional Granger Causality and Application to Multivariate Neural Field Potential Data. *Journal of Neuroscience Methods*, **150**, 228-237. https://doi.org/10.1016/j.jneumeth.2005.06.011

24. Pereda, E., Quiroga, R.Q. and Bhattacharya, J. (2005) Nonlinear Multivariate Analysis of Neurophysiological Signals. *Progress in Neurobiology*, **77**, 1-37. https://doi.org/10.1016/j.pneurobio.2005.10.003

25. Gong, G., He, Y. and Evans, A.C. (2011) Brain Connectivity: Gender Makes a Difference. *The Neuroscientist*, **17**, 575-591. https://doi.org/10.1177/1073858410386492